# *Development, characterization, and in vitro evaluation of phosphatidylcholine–sodium cholate-based nanoparticles for siRNA delivery to MCF-7 human breast cancer cells*

**Sebastián Ezequiel Pérez, Yamila Gándola, Adriana Mónica Carlucci & Lorena González**

**Journal of Nanoparticle Research**
An Interdisciplinary Forum for
Nanoscale Science and Technology

ISSN 1388-0764
Volume 17
Number 3

J Nanopart Res (2015) 17:1-15
DOI 10.1007/s11051-015-2937-1

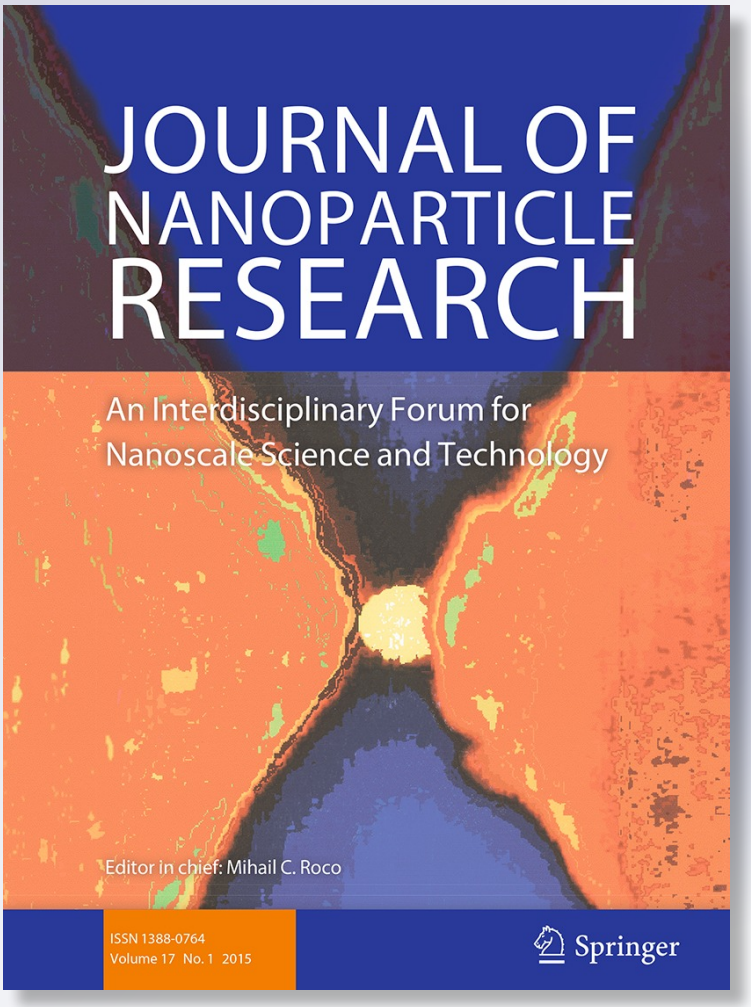


Springer

J Nanopart Res (2015) 17:128
DOI 10.1007/s11051-015-2937-1

RESEARCH PAPER

# Development, characterization, and in vitro evaluation of phosphatidylcholine–sodium cholate-based nanoparticles for siRNA delivery to MCF-7 human breast cancer cells

**Sebastián Ezequiel Pérez · Yamila Gándola · Adriana Mónica Carlucci · Lorena González**

Received: 19 November 2014 / Accepted: 28 February 2015


**Abstract** Phosphatidylcholine–sodium cholate (SC)-based nanoparticles were designed, characterized, and evaluated as plausible oligonucleotides delivery systems. For this purpose, formulation of the systems was optimized to obtain low cytotoxic vehicles with high siRNA-loading capacity and acceptable transfection ability. Mixtures of soybean phosphatidylcholine (SPC) and SC were prepared at different molar ratios with 2 % w/v total concentration; distilled water and two different buffers were used as dispersion medium. Nanoparticles below 150 nm were observed showing spherical shape which turned smaller in diameter as the SC molar proportion increased, accounting for small unilamellar vesicles when low proportions of SC were present in the formulation, but clear mixed micellar solutions at higher SC percentages. Macroscopic characteristics along with physicochemical parameters values supported the presence of these types of structures. SYBR green displacement assays demonstrated an important oligonucleotide binding that increased as bile salt relative content got higher. Within the same molar ratio, nanoparticles showed the following binding efficiency order: pH 7.4 > pH 5.0 > distilled water. siRNA-loading capacity assays confirmed the higher siRNA binding by the mixed micelles containing higher SC proportion; moreover, the complexes formed were smaller as the SC:SPC ratio increased. Considering cytotoxicity and siRNA-loading capacity, 1:2 and 1:4 SPC:SC formulations were selected for further biological assays. Nanoparticles prepared in any of the three media were able to induce dsRNA uptake and efficiently transfect RNA for gene silencing, for the compositions prepared in buffer pH 5.0 being the most versatile.

**Keywords** siRNA delivery system · Antisense therapy · Phosphatidylcholine–sodium cholate-based nanoparticles · Gene knockdown · Nanomedicine

## Introduction

RNA interference (RNAi) is a specific gene silencing mechanism that can be mediated by the delivery of chemically synthesized small interfering RNA (siRNA). The demonstration of this phenomenon in mammalian cells advised about its potential to be used for inhibiting the expression of any overexpressed protein involved in different pathologies, including

Sebastián Ezequiel Pérez and Yamila Gándola contributed equally to this paper.

S. E. Pérez (✉) · A. M. Carlucci
Department of Pharmaceutical Technology, Faculty of Pharmacy and Biochemistry, University of Buenos Aires, Junín 954, 1113AAD Buenos Aires, Argentina
e-mail: seperez@ffyb.uba.ar

Y. Gándola · L. González
Institute and Department of Biological Chemistry, Faculty of Pharmacy and Biochemistry, University of Buenos Aires, Junín 954, 1113AAD Buenos Aires, Argentina

Published online: 10 March 2015

cancer initiation and progression (de Fougerolles et al. 2007; Günther et al. 2011; Gomes-da-Silva et al. 2012). However, its limited cellular uptake, low biological stability, and unfavorable pharmacokinetics have limited its in vivo administration and therapeutical use as a new class of biological drug (Shim and Kwon 2010; Katas and Oya Alpar 2006; Wu et al. 2011; Schroeder et al. 2010).

The ideal in vivo delivery system for siRNA is expected to provide robust gene silencing, be biocompatible, biodegradable, and nonimmunogenic, and bypass rapid hepatic or renal clearance. Furthermore, an ideal delivery system should be able to actively target siRNA to the tumor (Ozpolat et al. 2010). Nanopharmaceutics are currently considered to be the most appropriate systems to fulfill these requirements. Their nanometric sizes naturally improve the cellular uptake; additionally, the enhanced permeability and retention (EPR) effect, typical in the intercellular tumor microenvironment, goes along with their increased biological action (Bosselmann and Williams 2012; Barenholz 2012; Khurana et al. 2010). The high cell tumor density and the stromal compaction can hinder the movement of drugs within the neoplastic tissue (Barenholz 2012; Cukierman and Khan 2010). However, the EPR effect could contribute to drug delivery from nanoparticles and macromolecules (Barenholz 2012).

Nowadays, scientific community claims for an increasing effort in rationale formulation design so as to obtain drug delivery systems with desirable pharmacotechnical characteristics; this means that efforts would be driven to more efficient, stable, ease-making, and safe dosage forms (Grobmyera et al. 2012; Schroeder et al. 2010; Shim and Kwon 2010; Günther et al. 2011). The complexity and multicomponent nature of some proposed nanomedicines is related to a number of additional variables that could further make the elaboration process control more difficult and the biological behavior evaluation as well (Barenholz 2012). Therefore, the translation of siRNA to the clinical setting is highly dependent on the development of an appropriate delivery system (Gomes-da-Silva et al. 2012; Nishikawa and Huang 2001). Non-viral vectors, which are typically based on cationic lipids or polymers, are preferred to viral vectors because of safety concerns. Nanoparticles such as liposomes, micelles, emulsions, and solid lipid nanoparticles have been used for siRNA delivery. Cationic lipids have been traditionally the most popular and widely used delivery systems (Lemke 2008). However, strong interaction with blood components, uptake by the reticuloendothelial system (RES), targeting-related issues, and potential toxicity for lung and other organs were associated with the use of these delivery systems (Dokka et al. 2000; Spagnou et al. 2004; Lv et al. 2006; Guo and Huang 2012). These types of effects can be diminished or avoided by altering the lipid chemical compositions or using mixtures of different kinds of lipids (Ozpolat et al. 2010).

Among the non-viral vectors, liposomes are by far the most advanced ones due to significant advantages: efficient interaction with lipidic cell membranes and enhanced endosomal escape; consequently, entrapped siRNA is more efficiently delivered. Furthermore, numerous safe and well-tolerated commercial liposomal products for human clinical use offer a large knowledge base and technical experience. Lipid-based and liposomal delivery systems for siRNA molecules have demonstrated their potential by fast entry and growth in clinical trial programs (Kapoor et al. 2012).

SNALPs (stable nucleic acid lipid particles) are a class of lipidic nanoparticles which is currently one of the most important liposomal-like formulations for siRNA carrying/delivery. Their key components are a cationic lipid and a "helper" lipid covered by PEG. Results indicated that they were able to assure efficient interaction with siRNA, endosomal escape, and sufficient stability for nanoparticle blood circulation. siRNA molecules related to hepatitis B replication, hypercholesterolemia (ApoB receptors) (Lammers et al. 2012; Manjunath and Dykxhoorn 2010), vascular endothelial growth factor (VEGF), and kinesin protein (KSP) were in vivo successfully targeted (Judge et al. 2009). However, the most advanced clinical trials are for local siRNA delivery, inhalatory route for respiratoire syncytial virus (ALN-RSV01) (Phase IIb) (Zamora et al. 2011), and intravitreal injection of PF-655 for macular degeneration (Phase II) (Gooding et al. 2012).

The current state of the art in nanomedicine asks for a minimum set of characteristics that must be evaluated and reported when these kind of delivery systems are used. These parameters include: size average and size distribution, morphology, dispersion state, physical and chemical properties, superficial area, and surface chemistry. They must all be known because they greatly contribute to in vivo biological activity of targeted (active or passive) nanoparticles.

On the other hand, the ideal nanomedicine has been associated with some specific requirements such as: (i) detailed understanding of critical components and their consequent interactions, (ii) identification of key characteristics that can be further considered as the processś specifications, (iii) feasibility to establish the relationship between components and nanocarrier structure with performance, (iv) ability to reproduce the specifications during manufacture conditions. Additionally, it is asked for ease of sterile production, ability to target and accumulate in the desired site of action overcoming the restrictions that biological barriers generally present, and an ultimate but prior condition—appropriate stability during the shelf life including storage and administration process.

Considering the state of art mentioned, the present work proposes the design of siRNA nanocarriers based on pharmaceutically acceptable excipients that could also be prepared by a relative simple technique. Phosphatidylcholine is one of the most important cell membrane constituents, it also represents the main component of lecithin (approximately 98 % w/w) and it has been extensively used in pharmaceutical industry for nanoemulsions, liposomes, and mixed micelles preparation. We have already reported the use of lecithin-based nanoparticles as siRNA drug delivery system (Pérez et al. 2012). On the other hand, bile salts are amphiphilic water-soluble molecules that have a characteristic chemical structure when compared with typical tensioactive compounds. In water, they are able to form micelles as well, but the behavior of bile salt-based micelles is significantly different from the tensioactive-based micelles. Bile salts are able to form small and charged micelles which show proper and distinctive structure; they form these micelles with a number of other water-soluble or insoluble lipid substances (Walter et al. 1991, 2000). Other pharmacotechnical advantages of their use are the thermodynamic stability of these micelles and their capacity to improve drug chemical stabilization (Dangi et al. 1998). Because of that, mixed micelles have been extensively studied with academic purposes and are currently marketed (Monteagudo et al. 2012) and used as drug delivery system. Thus, they have been studied for loading hydrophilic active compounds such as peptides (Hendradi et al. 2003) and proteins (US patent 6017545 A 2000); even though, and as far as our knowledge, they have not been used as oligonucleotides carriers until the moment. Moreover, the feasibility to formulate this type of nanocarrier with physical and chemical stability is possible; consequently, they present optimal technology transference potential at a reasonable cost, even if intravenous administration is the attempted route of administration (Naik et al. 2005).

The objective of the study was to design and characterize different phosphatidylcholine/bile salts-based nanoparticles formulations, in order to optimize the experimental conditions for their use as oligonucleotide delivery systems.

## Materials and methods

### Materials

Commercially available Stealth™ RNAi Actin Positive Control, BLOCK-iT™ Alexa Fluor Red Fluorescent Control, fluorescein-labeled dsRNA BLOCK-iT™ Fluorescent Oligo, and the transfection reagent Lipofectamine® RNAiMAX were obtained from Invitrogen (CA, United States). Soybean phosphatidylcholine (SPC) (Phospholipon® 90G) was purchased from Lipoid (Ludwigshafen, Germany). SYBR green I nucleic acid gel stain (10,000× concentrated in DMSO) and sodium cholate (SC) hydrate bioreagent were obtained from Sigma-Aldrich (Buenos Aires, Argentina). Highly purified water was used (Barnstead Easypure II, Thermo Scientific, USA). All other reagents were of analytical grade and used without further purification. MCF-7 human breast cancer cell line was obtained from the American Type Culture Collection (ATCC) (Rockville, MD, USA). Cells were maintained in Dulbecco's minimum essential medium (DMEM) supplemented with 10 % fetal bovine serum (FBS), 50 μg/mL gentamicine (Invitrogen Argentina), and 2 mM L-glutamine (Invitrogen Argentina). Cells were cultured in 75 $cm^2$ culture flasks at 37 °C in a humidified atmosphere of 5 % $CO_2$.

### Preparation of the formulations

Mixtures of SPC and SC were prepared at SPC:SC molar ratios of 1:1, 1:2, 1:4, and 1:8 to give clear micellar solutions with 2 % w/v total concentration—i.e., 2 g of SPC:SC (at the given ratios) every 100 mL of solution. These molar ratios were selected based on the extent of SPC solubilization by SC previously

reported by other authors (Hammad and Müller 1998; Dürr et al. 1994; Smidt et al. 1994). Different solvents (distilled water, 67 mM isotonic phosphate buffer pH 7.4, and 50 mM isotonic acetate buffer pH 5.0) were utilized as dispersion medium. Buffers were isotonized by adding sodium chloride when necessary according to Sörensen and White-Vincent methods. Weighted quantities of SPC, SC, and the appropriate solvent were mixed in a vial at 60 °C by the use of a thermostatic magnetic stirrer until fully dispersed. Next, the dispersions were stirred for 2 min at the same temperature with a high-shear mixer (Ultra-Turrax T25 basic, IKA Werke, Staufen, Germany) at 13,000 rpm and sonicated at 20 kHz and 50 W—30 % probe amplitude control—with an ultrasonic probe processor (Q700 Sonicator, QSonica LLC, Newtown CT, USA). The final formulations were filtrated through 0.45 μm PTFE Millipore filters and sealed into dark glass vials (Sznitowska et al. 2008). For siRNA loading, the empty nanoparticles were combined with siRNA, gently mixed, and incubated at room temperature for 20 min.

## Physical characterization of the size and surface charge of the particles

The particle size of the resulting particles was determined by photon correlation spectroscopy (PCS) using a Zetasizer (Malvern Nano ZS, Malvern Instruments Ltd., UK). Measurements were performed at 25 °C, collecting backscattered light at 173°. Each run underwent 12 subruns. The evaluations applied values of 0.89 cP and 1.33 for the viscosity and the refractive index of the solutions, respectively. The electrophoretic mobility of the samples was measured by the same instrument and the zeta ξ potential values were calculated according to Smoluchowski equation. Prior to analysis, particles were collected by ultracentrifugation (Eppendorf centrifuge 5415R, Hamburg, Germany) at 13,000×*g* for 10 min. The supernatants were discarded and nanoparticles were resuspended in distilled water.

## Morphology determined by transmission electron microscopy (TEM) and scanning electron microscopy (SEM)

The size and morphology of the particles, treated as previously described in "Physical characterization of the size and surface charge of the particles" section, were observed using a transmission electron microscope (TEM Philips EM 301) and a scanning electron microscope with field emission gun (Zeiss Supra 40) at the Advanced Microscopy Center (CMA) of the University of Buenos Aires.

For TEM analysis, one drop of sample was placed on a carbon-coated 200-mesh copper specimen grid and left to stand for 1.5 min, and all excess fluid was removed with filter paper. The grid was then stained with one drop of 1 % uranyl acetate solution (0.2 μm filtrated) for 30 s, and all excess of uranyl acetate was again removed with filter paper. The grid was allowed to dry at room temperature in a dust-free place before being examined. A negative uranyl acetate-stained blank was also performed. For SEM analysis, one drop of sample was deposited and dried on a silicon wafer and then coated with gold using an ion sputter.

## SYBR green displacement assay

The fluorescence intensity of SYBR green (10,000× diluted) in TE buffer (10 mM Tris–HCl, 1 mM EDTA, pH 8.0) was measured at an excitation wavelength of 485 nm and emission wavelength of 528 nm using a BioTek FLx800 fluorescence microplate reader (BioTek Instruments, USA). This was set at 0 % relative fluorescence, whereupon 10 pmol siRNA was added and the relative fluorescence was fixed at 100 %. Targeted particles were then added in 5 μL aliquots in a stepwise manner to the SYBR green-siRNA solution to a total of 50 μL and the relative fluorescence recorded at each stage. Preliminary tests were made in order to assure there were no signal variations due to formulation itself or stepwise dilution.

## Gel electrophoresis retardation studies

To evaluate the siRNA complex formation, a gel retardation assay was carried out by agarose gel electrophoresis. For this purpose, formulations were combined with 10 pmol of siRNA and incubated at room temperature for 20 min. Loading of siRNA was evaluated on 1 % agarose gel with Tris-acetate (TAE) running buffer at 100 V for 30 min. siRNA was visualized with ethidium bromide (0.5 μg/mL).

### Cell viability assay

MCF-7 cells were seeded in clear 96-well plates (Corning Costar, Fisher Scientific, USA) at a density of 10,000 cells/well. After 24 h, different concentrations of the unloaded nanoparticles ranging from 0.10 to 0.40 % w/v were added in 100 μl of medium. Cells were incubated at 37 °C for 48 h in a 5 % $CO_2$ atmosphere. Then medium was changed for fresh medium and the tetrazolium compound (CellTiter 96® aqueous non-radioactive cell proliferation assay, Promega) was added and manipulated according to the manufacturer's instructions. Absorbance was measured at 490 nm using an ELISA plate reader (Amersham Biosciences Biotrak II). Triplicates were run for each treatment. Values were expressed in terms of percent of untreated control cells set as 100 %.

### Intracellular delivery of fluorescent-labeled oligo

siRNA uptake was evaluated by transfection of the MCF-7 cells with two different fluorescent-labeled double-stranded RNAs (dsRNA): the BLOCK-iT™ Alexa Fluor® Red Fluorescent Oligo and the fluorescein-labeled dsRNA BLOCK-iT™ Fluorescent Oligo, both from Invitrogen. Transfection of the control dsRNA was performed following manufactureŕs recommendations. Fluorescent dsRNA (6 pmols) and the different formulations were mixed and incubated for 20 min to allow complex assemble. For control experiments, Lipofectamine® (1 μL) was also mixed with the dsRNAs (6 pmols) and assayed in parallel. After incubation, cells were seeded on 24-well plates at a density of $5 \times 10^4$ cells/well and incubated with the resulting complexes, the dsRNA:Lipofectamine® control complex or the dsRNA alone for 18 h at 37 °C in a $CO_2$ incubator. Afterward, cellular uptake was evaluated; for this purpose, cells were washed and fixed. To show the intracellular distribution of the siRNA, the nuclei were stained with Hoechst 33342 (1 μg/mL) for 15 min at 37 °C. Finally, the fluorescence signal was detected using fluorescence microscopy (Leica DM 2000 microscope).

### siRNA transfection assay

For transfection experiments, a control anti-actin siRNA (Stealth™ RNAi Actin Positive Control, Invitrogen) was used. The siRNA (60 pmols) and the different formulations were mixed and incubated for 20 min to allow complex assemble. For control experiments, Lipofectamine® (3 μL) was also mixed with the siRNA (60 pmols) and assayed in parallel. After incubation, cells were seeded on 24-well plates at a density of $5 \times 10^4$ cells/well and incubated with the resulting complexes for 18 h at 37 °C in a $CO_2$ incubator. Afterwards, transfection medium was replaced by fresh growth medium and cells were further incubated for 48 h. Actin silencing was evaluated by phalloidin staining which was detected by fluorescence microscopy (Leica DM 2000 mycroscope).

### Statistical analyses

Statistical analyses were carried out using one-way analysis of variance (ANOVA) in GraphPad InStat 3.01 for Windows. A $p$ value of $\leq 0.05$ (two-tailed) was considered to be statistically significant.

## Results and discussion

### Physico-chemical characterization of the nanoparticles

Size and surface charge of both, the unloaded particles and the siRNA-loaded formulations were determined by dynamic light scattering (DLS). As shown in Table 1, particles in the range of 80–150 nm were readily obtained for the 1:1 and 1:2 water, 1:1 and 1:2 pH 5.0 and 1:1 pH 7.4 systems. Meanwhile, particles ranging 10–70 nm were obtained in the other cases. Average size distributions for the evaluated formulations were obtained with low polydispersity in general, accounting for quite homogeneous nanoparticles' populations except for some water and 1:2 compositions. TEM and SEM images of the particles are presented in Fig. 1a, b; the results correlate with the findings by DLS measurements, showing spherical shape particles which turn smaller in diameter as the SC molar proportion increases.

The values obtained for $\xi$ potential were negative for all the formulations (from −7 to −30.9 mV), not only for the empty formula but also for the siRNA-loaded ones, as it was expected because of their compositions. Moreover, almost all the compositions, except ratio 1:8 at pH 5.0 and ratio 1:2 at pH 7.4, showed a significant decrease in their value after

**Table 1** Particle size and zeta $\xi$ potential of the unloaded and siRNA-loaded nanoparticles

| SPCSC ratio | Unloaded particles | | | siRNA-loaded particles | | |
|---|---|---|---|---|---|---|
| | Particle size (d. nm) | Pdl | *Z*-pot (mV) | Particle size (d. nm) | Pdl | *Z*-pot (mV) |
| Water | | | | | | |
| 1:1 | 135.5 ± 2.0 | 0.272 | −26.1 ± 1.6 | 143.2 ± 4.1 | 0.279 | −37.8 ± 1.6 |
| 1:2 | 126.8 ± 1.1 | 0.380 | −30.9 ± 1.5 | 142.3 ± 3.7 | 0.237 | −44.4 ± 2.1 |
| 1:4 | 7.9 ± 0.1 | 0.432 | −15.7 ± 4.2 | 17.4 ± 5.8 | 0.481 | −23.6 ± 4.5 |
| 1:8 | 6.6 ± 0.2 | 0.761 | −8.1 ± 3.4 | 7.2 ± 0.2 | 0.705 | −18.3 ± 0.8 |
| pH 5.0 | | | | | | |
| 1:1 | 128.7 ± 1.9 | 0.284 | −14.9 ± 0.7 | 104.9 ± 3.1 | 0.268 | −21.3 ± 0.9 |
| 1:2 | 103.9 ± 3.1 | 0.691 | −15.8 ± 2.0 | 125.8 ± 1.5 | 0.135 | −22.4 ± 2.7 |
| 1:4 | 23.7 ± 0.7 | 0.204 | −8.8 ± 8.1 | 22.7 ± 0.6 | 0.179 | −16.0 ± 0.7 |
| 1:8 | 56.3 ± 1.5 | 0.264 | −8.7 ± 7.3 | 20.5 ± 0.5 | 0.066 | −6.4 ± 1.1 |
| pH 7.4 | | | | | | |
| 1:1 | 122.3 ± 3.4 | 0.244 | −18.3 ± 2.3 | 85.2 ± 3.4 | 0.231 | −27.1 ± 1.8 |
| 1:2 | 69.9 ± 3.7 | 0.424 | −22.6 ± 3.6 | 23.1 ± 0.5 | 0.289 | −11.5 ± 1.1 |
| 1:4 | 21.9 ± 0.4 | 0.099 | −8.9 ± 3.9 | 21.2 ± 0.9 | 0.312 | −16.3 ± 1.5 |
| 1:8 | 44.5 ± 4.5 | 0.321 | −7.0 ± 2.2 | 39.2 ± 1.4 | 0.242 | −18.7 ± 3.7 |

Data shown are mean ± SD ($n = 4$)

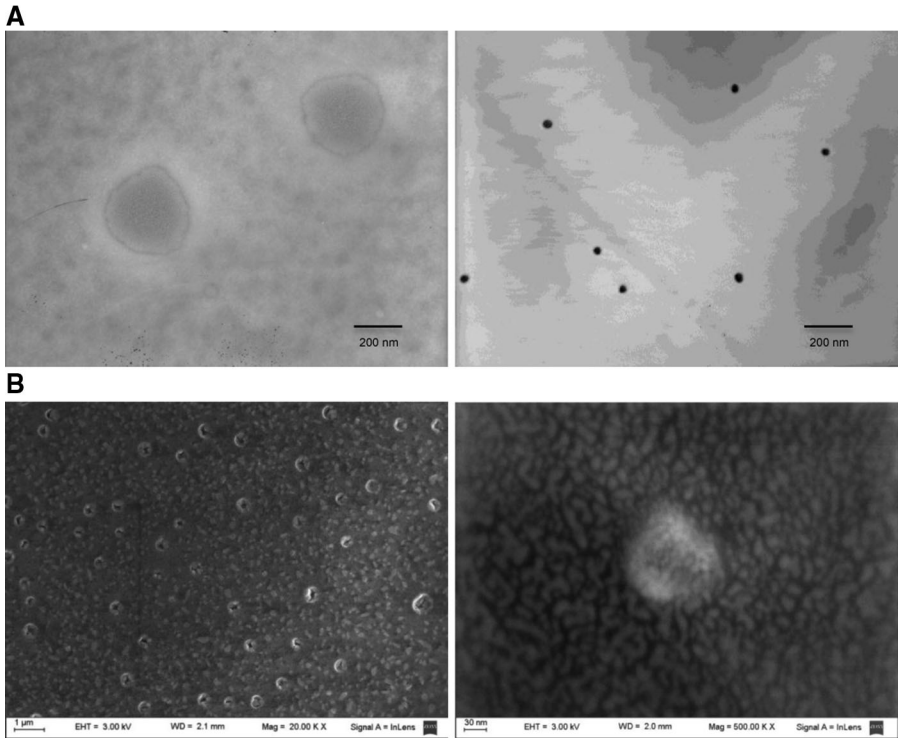


**Fig. 1** Transmission electron micrographs (**a**) and scanning electron micrographs (**b**) of the siRNA-loaded pH 5.0 SPC:SC 1:1 (*left*) and SPC:SC 1:8 (*right*) formulations


**Fig. 2** Unloaded formulations: from *left* to *right*, SPC:SC 1:1, 1:2, 1:4, and 1:8 in water (**a**), pH 5.0 buffer (**b**), and pH 7.4 buffer (**c**)

siRNA loading with final values ranging from −6.4 to −44.4 mV.

It is well known that the size, structure, and composition of aggregates in phospholipids-bile salt mixtures depend on the ratio of bile salts to phospholipid (Müller 1981). Walter et al. (1991) measured the turbidity by light scattering as an indirect indicator of the microstructural changes of the lipid-containing aggregates during the continuous addition of cholate to a cuvette containing PC sonicated vesicles; the changes were then confirmed by cryo-TEM images (Walter et al. 1991). This work concluded that PC forms bilayer structures when dispersed in aqueous solution at high water content and that if enough cholate is added to a suspension of PC vesicles, the dispersion becomes clear, indicating that the structures turn to smaller ones; most of the structures appear as uniform tiny dots, indicative of spheroidal micelles.

More recently, (Chen et al. 2008) have described that mixtures of phospholipids and surfactants such as the bile salts form mixed amphiphile structures, the nature of which depends on the relative amounts of phospholipids and surfactant. This work also clearly established that at high surfactant-to-phospholipid ratios, small micelles are formed. At very low ratios, the predominant amphiphile, the phospholipids, forms bilayer membrane vesicles with some surfactant incorporated. Because of that, mixed micelles are formed at high ratios while vesicles are formed at very low ratios (Chen et al. 2008). Moreover, Venneman et al. (2002) have reported that the phospholipid bilayer is disintegrated and mixed micelles are formed when phospholipid vesicles interact with bile salts at high concentration (a ratio of bile salts to phospholipid ≥4) (Venneman et al. 2002).

It can be proposed, then, that when low proportions of SC are present in the formulation small unilamellar vesicles are formed, whereas high percentages of SC lead to the formation of clear mixed micellar solutions instead. This can also explain the macroscopic differences among the preparations, showing low turbidity when vesicles are present, but total transparence when mixed micelles are the predominant structures. It is also interesting to remark that even the systems presenting vesicle structures showed no flocculation (Fig. 2), meaning they can be considered stable systems as well. This fact would be in agreement with the above 15 mV $\xi$ potential absolute values obtained, making it reasonable to expect acceptable colloidal stability due to dominant repulsive forces (Table 1). Although no clear correlation could be found between siRNA loading and the particles size, it can be seen that already negatively charged unloaded particles tend to slightly decrease their zeta potential upon siRNA addition, which could indicate that the location of the oligonucleotide is at least in part on the surface of the particles (Omedes Pujol et al. 2013).

Encapsulation of siRNA into liposomes can be achieved during liposome preparation or after liposome preparation. It has been described that siRNA entrapment after liposome preparation occurs as a result of lipid–siRNA electrostatic interactions, followed by the lipid layers restructuring (Kapoor et al. 2012). Nanoparticle siRNA entrapment might occur as a result of lipid–siRNA interactions and reorganization of the nanoparticle structure as well. Meanwhile, the tendency to show more negative $\xi$ potential values after siRNA addition is an important fact supporting that siRNA molecules mainly locate on the external surface of the nanoparticles.

## Association of the duplex RNA with formulated nanoparticles

In order to evaluate siRNA-loading capacity, binding efficiency between the oligonucleotide and the different developed formulations (SPC:SC molar ratios ranging from 1:1 to 1:8 prepared in different dispersion media) was established by means of a high-sensitivity fluorescence displacement assay (Figs. 3, 4). The assay is based on SYBR green displacement from siRNA by increasing amounts of the targeted vehicles (Dorasamy et al. 2009; Sun et al. 2009; Geall and Blagbrough 2000). The attendant reduction in SYBR green fluorescence following dissociation from the nucleic acid is followed in a spectrofluorometer during the stepwise addition of the systems. It can be seen that values are reached beyond which further additions of the formulated systems, i.e., getting to higher N/P ratios—ratio between the phosphatidylcholine molecules (one amine group per molecule) and the phosphate groups present in siRNA (42 phosphate groups per molecule)—do not lead to significant further loss of fluorescence; these mark the maximum SYBR green displacement and the complete vehicle association of the siRNA (Zhao et al. 2009).

Results demonstrated an important binding between siRNA and each formulation, considerably increasing as SC relative content gets higher (Fig. 3). Increased siRNA binding to MM containing higher SC proportion might account on the smaller negative net charge associated with the surface of these particles. However, the consideration of differences regarding charges would not be appropriate as differences in size is another important parameter; smaller particles could present a more convenient size/charge ratio to bind siRNA, which could justify the increased loading capability of the SPC:SC mixed micelles with higher SC proportions. When results are presented in a different graphical configuration, it can be clearly seen that within the same SPC:SC molar ratio the siRNA binding is higher in pH 7.4 than in pH 5.0 isotonic formulations, and much higher than in those dispersed in distilled water (Fig. 4). It could be suggested that the presence of salts in the isotonic media collaborates to increase the ionic strength of the medium, being well known that the higher the ionic strength of the medium, the lower the critical micelle concentration, accounting for the ease and quality of the particles obtained.

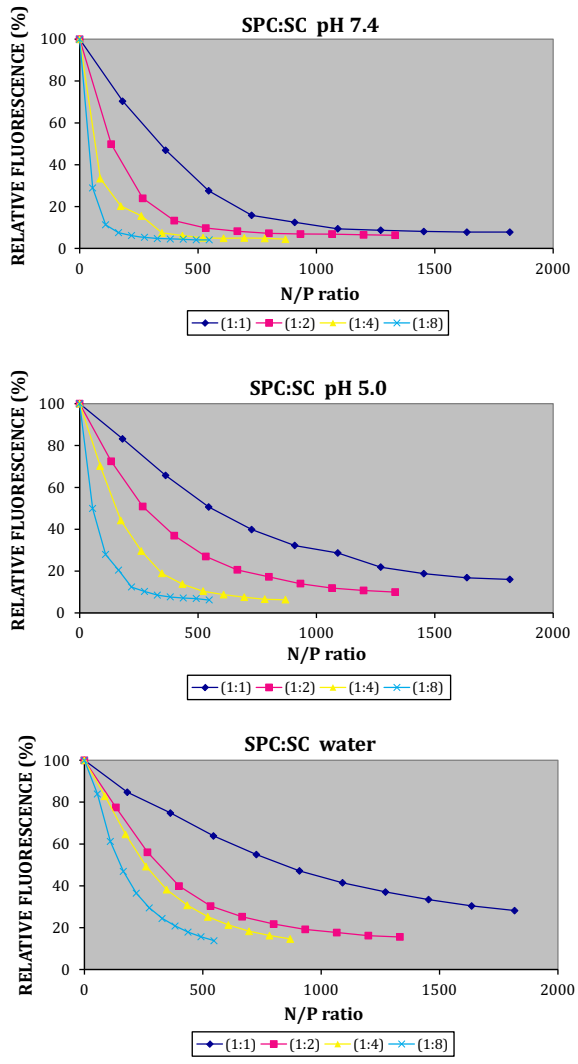


**Fig. 3** SYBR green displacement assay comparing binding efficiency between the oligonucleotide and the different SPC:PC formulations in each dispersion medium

Results from the fluorescence displacement assay were then correlated with observations from band shift assays. To compare the siRNA-loading capability of the different mixed micelles prepared in the various buffers, analysis was performed at the same N/P ratio. Previously, a series of different mixed micelles: siRNA weight ratios have been prepared and incubated for each formulation to determine the N/P 500 ratio as appropriate for comparison. Moreover, results from the fluorescence displacement assay demonstrated a

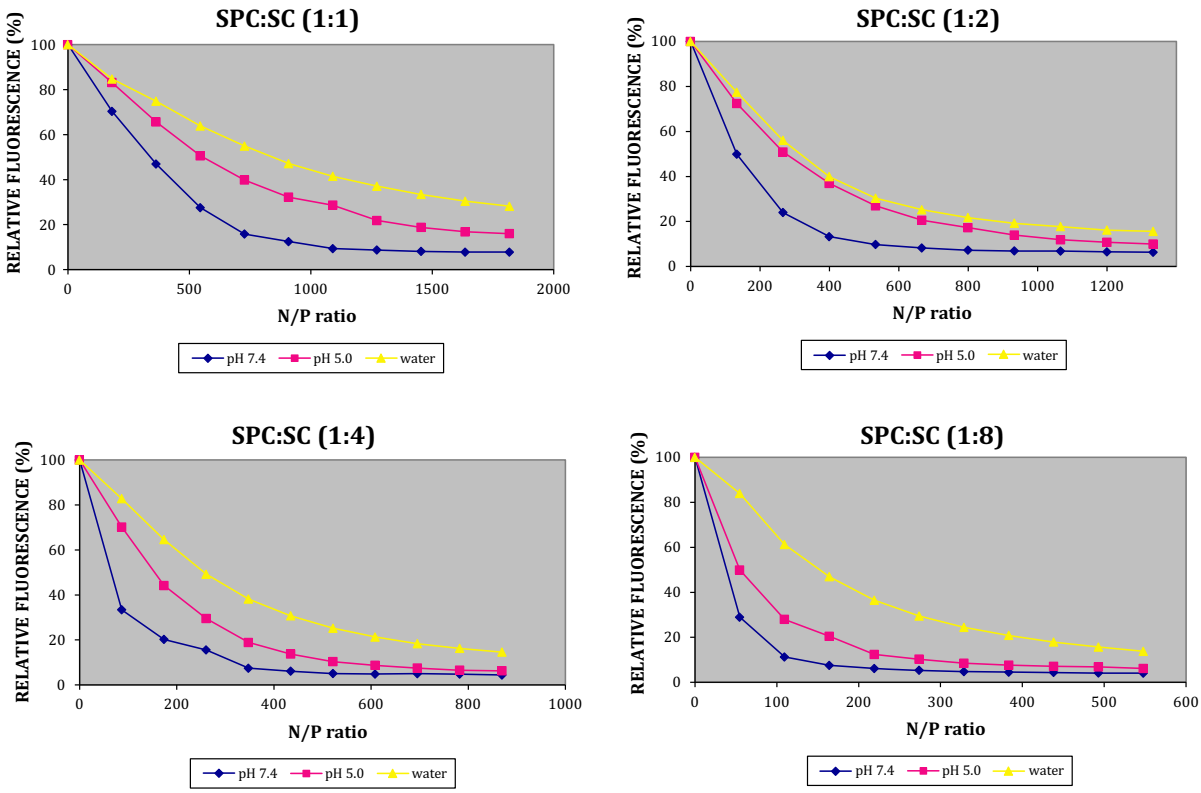


**Fig. 4** SYBR green displacement assay comparing binding efficiency between the oligonucleotide and the different formulations within each SPC:PC molar ratio

significant binding capacity at this N/P ratio for every formulation.

As it is shown in Fig. 5, little siRNA loading is obtained when 1:1 mixed micelles are used; however, complex assembly increases as SPC:SC molar ratio rises. Furthermore, size of the complexes formed seems to diminish as the SPC:SC molar ratio rises. These observations confirm that the results obtained from the physico-chemical characterization, accounting for the formation of SPC:SC vesicles which turn into smaller, low-MW mixed micelles as the ratio of bile salts to phospholipid is higher. Noteworthy, the complex formed between siRNA and mixed micelles are smaller than the complex formed with lipofectamine in every case.

## Evaluation of SPC:SC formulations cytotoxicity

Cytotoxicity of many nanoparticle-based gene delivery systems limits their therapeutic application. MTS assays were performed to evaluate the remaining viability of cells treated with the nanoparticles plausible of being used as siRNA delivery systems. Considering the low siRNA-loading capacity of the 1:1 systems, these were no longer evaluated. On the other hand, the 1:2, 1:4, and 1:8 formulations prepared in the different solubilization media were assayed in different concentrations. As shown in Fig. 6, cytotoxicity of the mixed micelles increases as cholic acid proportion in the preparation augments; as a consequence, the 1:8 mixed micelles resulted to be the most toxic. Results are in accordance with previous findings demonstrating that lechithin attenuates cytotoxic effects of cholic acids (Tan et al. 2013). Regarding the solubilization medium, mixed micelles prepared in pH 5.0 buffer resulted with the least cytotoxic. The analysis of this phenomenon could be in relation to two different aspects, in first instance: (i) the ionization behavior of the nanoparticleś components, mainly the bile salt and (ii) the biological changes induced by the nanoparticles themselves. Cabral et al. have early demonstrated the broad range within apparent pKás of

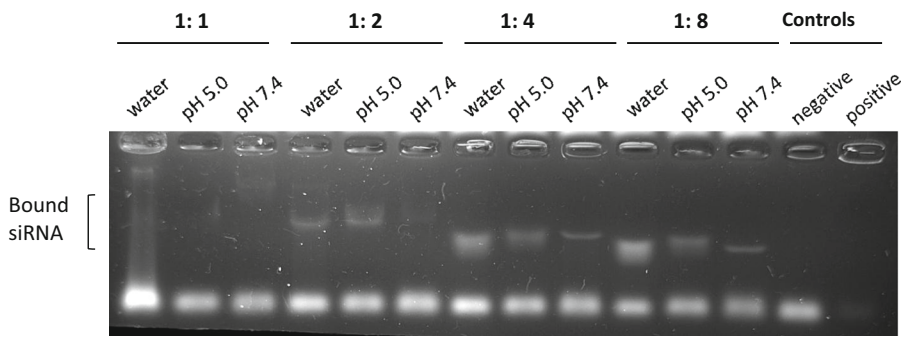


**Fig. 5** Gel retardation assay of siRNA incubated with the various SPC:SC molar ratio formulations (1:1, 1:2, 1:4, and 1:8) prepared in different diluents (water, pH 5.0, and pH 7.4 buffers). Control assay involved siRNA alone (−) or associated to Lipofectamine (+). (*Upper bands*: bound siRNA)

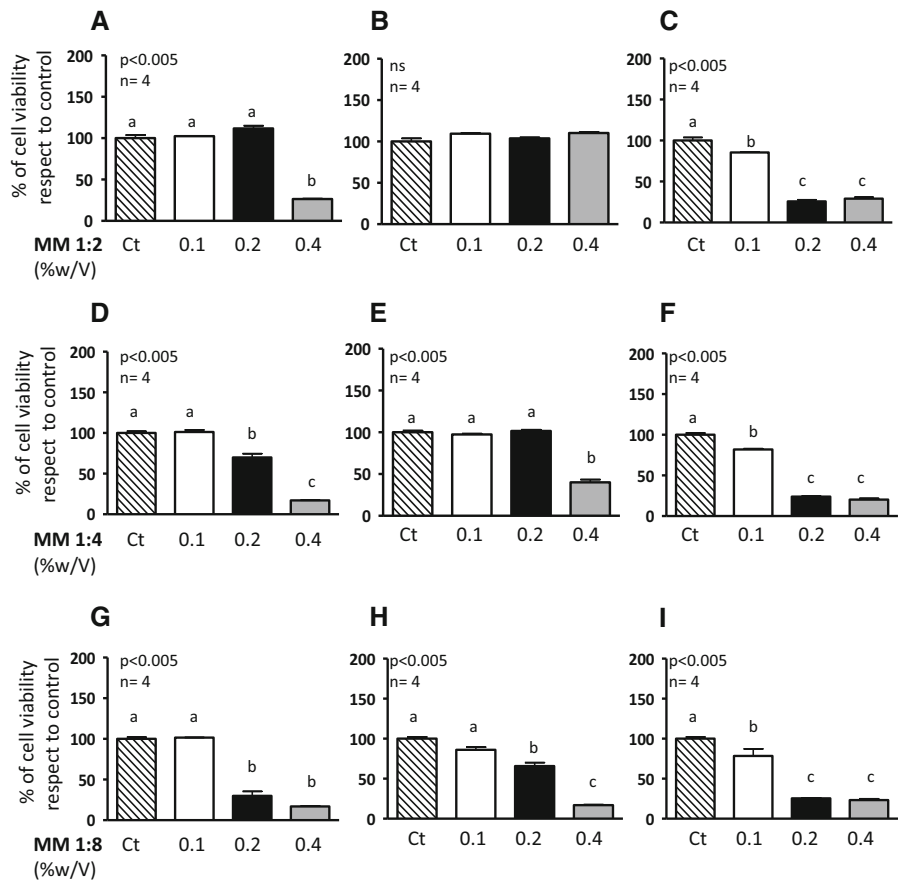


**Fig. 6** Viability of MCF-7 breast cancer cells incubated with the 1:2, 1:4, and 1:8 mixed micelles prepared at different %w/v in water, pH 5.0, and pH 7.4 buffers. Breast cancer cells were incubated for 48 h with the mixed micelles dispersed in water (**a**, **d**, and **g**), pH 5.0 buffer (**b**, **e**, and **h**), pH 7.4 buffer (**c**, **f**, and **i**), or vehicle (Ct). After incubation, cell viability was evaluated using the CellTiter 96 aqueous non-radioactive cell proliferation assay (Promega). Values were expressed in terms of percent of untreated control cells set as 100 %. Data are expressed as the mean ± S.E.M. of the indicated number (*n*) of independent experiments. Statistical analysis was performed by ANOVA. *Different letters* denote significant difference at $P < 0.05$, whereas results with the *same letter* are not statistically different from each other

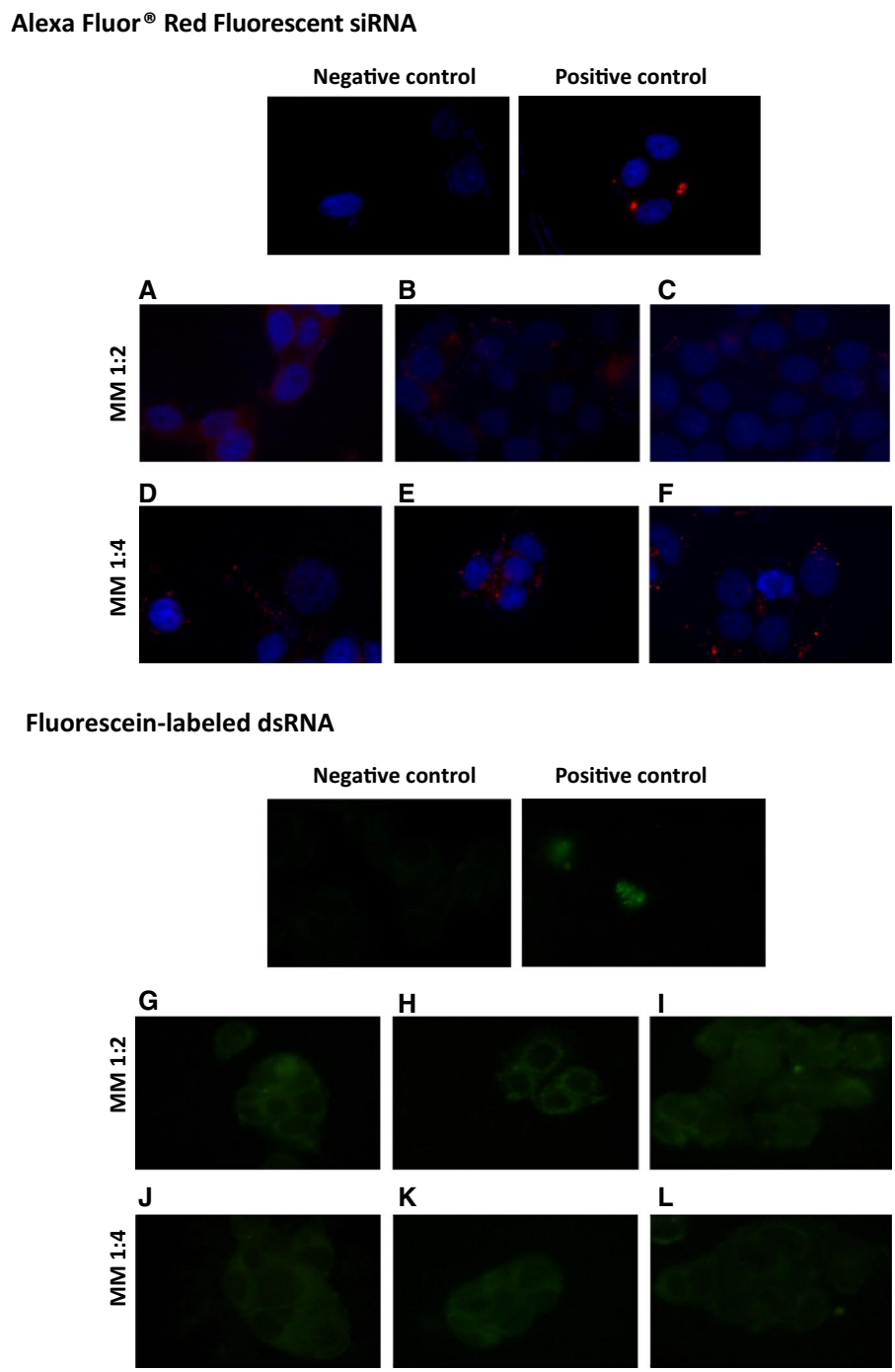


**Fig. 7** Fluorescent-labeled double-stranded RNAs (dsRNA) (BLOCK-iT™ Alexa Fluor® Red Fluorescent Oligo, Invitrogen) and fluorescein-labeled dsRNA BLOCK-iT™ Fluorescent Oligo were used to visualize the cellular uptake and subcellular localization of the mixed micelles:dsRNA complexes. MCF-7 breast cancer cells incubated only with the fluorescent oligos (*negative controls*), lipofectin/fluorescent oligos (*positive controls*), mixed micelles 1:2/Alexa Fluor® Red Fluorescent siRNA (**a**, **b**, and **c**), mixed micelles 1:4/Alexa Fluor® Red Fluorescent siRNA (**d**, **e**, and **f**), mixed micelles 1:2/Fluorescein-labeled dsRNA (**g**, **h**, and **i**), or mixed micelles 1:4/Fluorescein-labeled dsRNA (**j**, **k,** and **l**). Mixed micelles prepared in the different solubilization media were assayed: water (**a**, **d**, **g**, and **j**), pH 5.0 buffer (**b**, **e**, **h**, and **k**), and pH 7.4 buffer (**c**, **f**, **i**, and **l**). For microscopy visualization cells were washed, fixed, and incubated with Hoechst (only **a**–**f**). Representative images of control and mixed micelles-treated cells are shown

bile acids in different molecular environments; for cholic acid these values ranged from 4.6 (below the critic micellar concentration) to 7.3 (for bile acid/egg PC vesicles in ratio 3:97 w/w) (Cabral et al. 1986). On the other hand, we have previously studied the effects of PC-based nanoparticles over breast cancer cellular proliferation and signaling. Results suggested that nanoparticles were able to induce physico-chemical changes in the plasma membrane of cancer cells with a correlation in biological behavior, such as EGFR

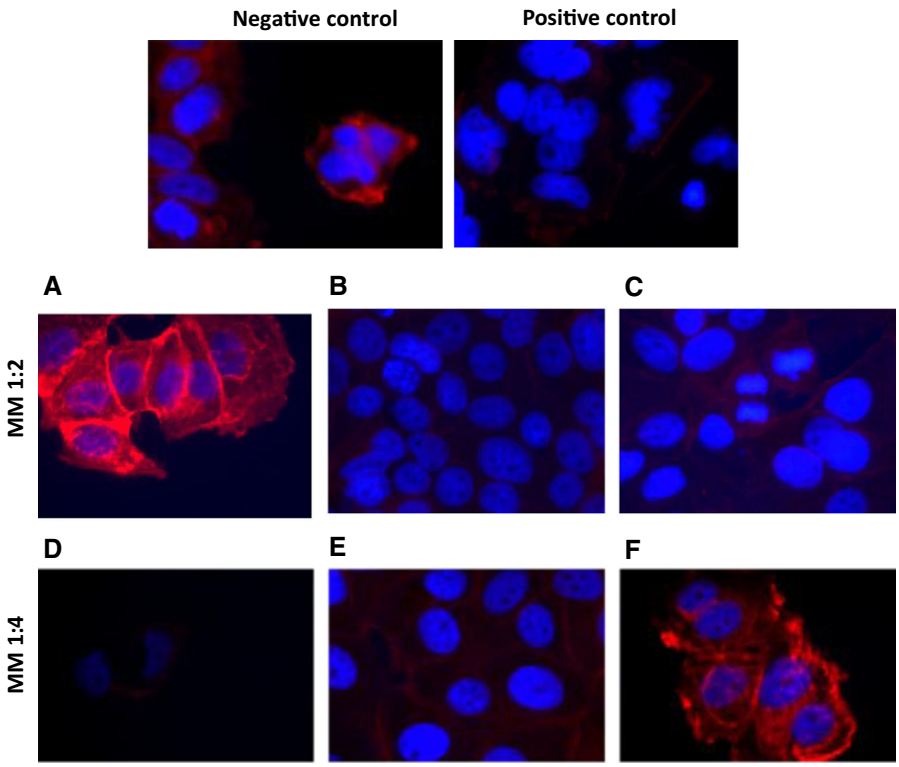


**Fig. 8** Phalloidin staining of MCF-7 breast cancer cells incubated with naked siRNA (*negative control*), lipofectain/anti-actin siRNA (*positive control*), mixed micelles 1:2/anti-actin siRNA (**a**, **b**, **c**), or mixed micelles 1:4/anti-actin siRNA (**d**, **e**, **f**). Mixed micelles prepared in the different solubilization media were assayed: water (**a** and **d**), pH 5.0 buffer (**b** and **e**), and pH 7.4 buffer (**c** and **f**). For actin immunocytochemistry, transfected cells were washed, fixed, permeabilized, blocked, and incubated with phalloidin and Hoechst. Finally covers were mounted and examined by epifluorescence microscopy. Representative merged images of control and mixed micelles-treated cells are shown

cellular localization and/or activity inducing proliferation (Gándola et al. 2014).

Considering cytotoxicity and siRNA-loading capacity, 1:2 and 1:4 SPC:SC formulations were selected to asses their ability to deliver fluorescent dsRNA into the cells and efficiently trigger siRNA-mediated gene silencing.

## Intracellular delivery of fluorescent-labeled oligo and gene knockdown

Two different fluorescent-labeled double-stranded RNAs (dsRNA), the BLOCK-iT™ Alexa Fluor® Red Fluorescent Oligo, and the fluorescein-labeled dsRNA BLOCK-iT™ Fluorescent Oligo (Invitrogen) were used to visualize the cellular uptake of the nanoparticle:dsRNA complexes (Fig. 7). Control experiments were performed in parallel; in order to assess unspecific fluorescence and association of the dsRNA to cells, fluorescent oligos were incubated in the absence of a delivery system with the MCF-7 cells (negative control); and efficient delivery of the fluorescent oligo was assessed by delivery with a commercially available transfection medium recommended for dsRNA transfection (positive control). As it can be observed in Fig. 7, both fluorescently labeled dsRNAs were internalized by a significant proportion of cells even when associated with lipofectamine (positive control) or the nanoparticles. In contrast, fluorescently labeled naked dsRNA was not detected within cells or in the extracellular medium (negative control). Alexa Fluor® Red Fluorescent Oligo was mainly located in the cytoplasm of the cells near the nucleus (positive control, Fig. 7a–f) according to the previous studies performed with the lechitin nanoparticles (Pérez et al. 2012); however, fluorescein-labeled

dsRNA was evidenced in the nucleus and perinuclear region (positive control, Fig. 7g–l) as previously described (Fisher et al. 1993). Cellular uptake of fluorescent oligos is not a reliable quantitative technique to compare efficiency between the different formulations; however, the ability of the vehicles to deliver the oligonucleotids was probed.

To investigate the efficiency of the pre-selected SPC:SC vehicles to deliver siRNA and silence target genes, the RNAi-mediated silencing of actin expression by the nanoparticle/siRNA complexes was examined in cultured cells. Nanoparticles at 1:2 and 1:4 SPC:SC ratio were evaluated considering their acceptable capacity to bind siRNA and low cytotoxicity. The optimal siRNA concentration for actin silencing was previously evaluated by transfection assays with lipofectamine (positive control). Efficient siRNA activity was assessed by phalloidin staining of MCF-7 transfected cells. As shown in Fig. 8, naked siRNA showed no gene silencing effect (negative control), due to the enzymatic degradation in the FBS-containing medium as well as the restricted cellular uptake caused by the electrostatic repulsion against the negatively charged cellular membranes. In contrast, lipofectain/siRNA exerted an evident gene silencing effect (positive control). Effect of formulations was dependent on the SPC:SC ratio as well as on the diluents. Nanoparticles prepared at 1:2 SPC:SC showed a clear silencing of actin expression when prepared in buffers at pH 5.0 or pH 7.4, but not when prepared in water. Nanoparticles prepared at 1:4 SPC:SC ratio evidenced a significant silencing of actin when the diluents were water or the pH 5.0 buffer. To summarize, formulations 1:2 and 1:4 of the phosphatidylcholine/bile salts-based nanoparticles prepared in water, pH 5.0 or pH 7.4 buffers demonstrated to effectively bind siRNA; they can be used for transfection assays in a broad range of concentrations given their low cytotoxicity; are able to induce dsRNA uptake; and efficiently transfect RNA for gene silencing, for being the ones prepared in pH 5.0 buffer the most versatile.

## Conclusions

In the present work, a detailed physico-chemical characterization of the proposed nanoparticles was performed; a parallel functional biologic evaluation was also carried out so as to correlate results. In consequence, the oligo delivery systems used in this work are well characterized, imply simple preparation techniques, and are quite versatile. The delivery systems and transfection conditions were optimized in order to achieve lipid-based nanoparticles that were able to load siRNA and promote its delivery to the cells; moreover, cytotoxicity was minimized and efficiency to silence a target gene was proved in comparison with a well-recognized transfection agent which implies a second-generation lipid-based system.

In addition, high feasibility for technological transference was considered from the very beginning of the pharmaceutical development, because mixed micelles have already reached the market as vehicles for small chemical entities. An accessible cost of production was assured in parallel with the selection of this delivery system. Finally, it is remarkable that the present proposal follows the current trend to evaluate lipid-based nanoparticles as non-viral siRNA-loading/delivery systems, making focus on the selection of appropriate and well-known lipids to shorten the distance to successful in vivo use.

Further in vivo assays would help to define the required doses for intra-tumoral mixed micelles injections, and it would also enable the comparison of silencing efficiency for different siRNA targets involved in cancer promotion and progression. The silencing of these genes and their related therapeutic effects would be assayed through tumor growth reduction or period of extended survival.

**Acknowledgments** Support for these studies was provided by the National Agency of Scientific and Technological Promotion (ANPCyT), Ministry of Science, Technology, and Productive Innovation, Argentina, the University of Buenos Aires, and the National Science Research Council (CONICET). The authors have no relevant financial involvement with any organization or entity with a financial interest in or financial conflict with the subject matter or materials discussed in the manuscript. No writing assistance was utilized in the production of this manuscript.

## References

Barenholz Y (2012) Doxil®—The first FDA-approved nano-drug: lessons learned. J Control Release 160:117–134

Bosselmann S, Williams RO (2012) Has nanotechnology led to improved therapeutic outcomes? Drug Dev Ind Pharm 38:158–170

Cabral DJ, Hamilton JA, Small DM (1986) The ionization behavior of bile acids in different aqueous environments. J Lipid Res 27:334–344

Chen H, Guo Z, Yu F, Ki J et al (2008) Influence of La3+ ions on the egg-yolk phosphatidylcholine and sodium taurocholate self-assemblies in aqueous suspension. J Colloid Interface Sci 328:158–165

Cukierman E, Khan DR (2010) The benefits and challenges associated with the use of drug delivery systems in cancer therapy. Biochem Pharmacol 80:762–770

Dangi JS, Vyas SP, Dixit VK (1998) Effect of various lipid-bile salt mixed micelles on the intestinal absorption of Amphotericin-B in rat. Drug Dev Ind Pharm 24(7):631–635

de Fougerolles A, Vornlocher HP, Maraganore J, Lieberman J (2007) Interfering with disease: a progress report on siRNA-based therapeutics. Nat Rev Drug Discov 6(6):443–453

Dokka S, Toledo D, Shi X, Castranova V, Rojanasakul Y (2000) Oxygen radical-mediated pulmonary toxicity induced by some cationic liposomes. Pharm Res 17:521–525

Dorasamy S, Moganavelli S, Ariatti M (2009) Rapid and sensitive fluorometric analysis of novel galactosylated cationic liposome interaction with siRNA. Afr J Pharm Pharmacol 3:632–635

Dürr M, Hager J, Lohr JP (1994) Investigation on mixed micelle and liposome preparations for parenteral use based on soya phosphatidylcholine. Eur J Pharm Biopharm 40:147–156

Fisher TL, Terhorst T, Cao X, Wagner RW (1993) Intracellular disposition and metabolism of fluorescently-labeled unmodified and modified oligonucleotides microinjected into mammalian cells. Nucleic Acids Res 21:3857–3865

Gándola Y, Pérez SE, Irene PE, Sotelo AI, Miquet JG, Corradi GR, Carlucci AM, González L (2014) Mitogenic effects of phosphatidylcholine nanoparticles on MCF-7 breast cancer cells. Biomed Res Int. Vol 2014, Article ID 687037, p 13. doi: 10.1155/2014/687037

Geall AJ, Blagbrough IS (2000) Rapid and sensitive ethidium bromide fluorescence quenching assay of polyamine conjugate-DNA interactions for the analysis of lipoplex formation in gene therapy. J Pharm Biomed Anal 22:849–859

Gomes-da-Silva LC, Fonseca NA, Moura V, Pedroso de Lima MC, Simões S, Moreira JN (2012) Lipid-based nanoparticles for siRNA delivery in cancer therapy: paradigms and challenges. Acc Chem Res 45(7):1163–1171. doi:10.1021/ar300048p

Gooding M, Browne LP, Quinteiro FM, Selwood DL (2012) siRNA delivery: from lipids to cell-penetrating peptides and their mimics. Chem Biol Drug Des 80:787–809

Grobmyera SR, Zhoua G, Gutweina LG, Iwakumab N, Sharmac P, Hochwald SN (2012) Nanoparticle delivery for metastatic breast cancer. Nanomedicine 8:S21–S30

Günther M, Lipka J, Malek A, Gutsch D, Kreyling W et al (2011) Polyethylenimines for RNAi-mediated gene targeting in vivo and siRNA delivery to the lung. Eur J Pharm Biopharm 77:438–449

Guo X, Huang L (2012) Recent advances in nonviral vectors for gene delivery. Acc Chem Res 45(7):971–979. doi:10.1021/ar200151m

Hammad MA, Müller BW (1998) Increasing drug solubility by means of bile salt–phosphatidylcholine-based mixed micelles. Eur J Pharm Biopharm 46(3):361–367

Hendradi E, Obata Y, Takayama K, Nagai T (2003) Effect of bile salts-lecithin mixed micelles on the skin permeation of diclofenac in rats. STP Pharm Sci 13(4):247–251

Judge AD, Robbins M, Tavakoli I, Levi J, Hu L et al (2009) Confirming the RNAi-mediated mechanism of action of siRNA-based cancer therapeutics in mice. J Clin Invest 119(3):661–673

Kapoor M, Burgess DJ, Patil SD (2012) Physicochemical characterization techniques for lipid based delivery systems for siRNA. Int J Pharm 427:35–57

Katas H, Oya Alpar H (2006) Development and characterization of chitosan nanoparticles for siRNA delivery. J Control Release 115(2):216–225

Khurana B, Goyal AK, Budhiraja A, Arora D, Vyas SP (2010) siRNA delivery using nanocarriers—an efficient tool for gene silencing. Curr Gene Ther 10(2):139–155

Lammers T, Kiessling F, Hennink WE, Storm G (2012) Drug targeting to tumors: principles, pitfalls and (pre-) clinical progress. J Control Release 161:175–187

Lemke TL (2008) Pharmaceutical biotechnology: from nucleic acids to personalized medicine. In: (ed) Foye's principles of medicinal chemistry, 6th edn. Lippincott Williams & Wilkins, Philadelphia, pp 115–175

Lv H, Zhang S, Wang B, Cui S, Yan J (2006) Toxicity of cationic lipids and cationic polymers in gene delivery. J Control Release 114(1):100–109

Manjunath N, Dykxhoorn DM (2010) Advances in synthetic siRNA delivery. Discov Med 9(48):418–430

Monteagudo E, Gándola Y, González L, Bregni C, Carlucci A (2012) Development, characterization and in vitro evaluation of tamoxifen microemulsions. J Drug Deliv. Vol 2012, Article ID 236713, p 11. doi:10.1155/2012/236713

Müller K (1981) Structural dimorphism of bile salt/lecithin mixed micelles. A possible regulatory mechanism for cholesterol solubility in bile? X-ray structure analysis. Biochemistry 20:404–414

Naik S, Chougule M, Padhi BK, Misra A (2005) Development of novel lyophilized mixed micelle amphotericin B formulation for treatment of systemic fungal infection. Curr Drug Deliv 2(2):177–184

Nishikawa M, Huang L (2001) Nonviral vectors in the new millennium: delivery barriers in gene transfer. Hum Gene Ther 12(8):861–870

Omedes Pujol M, Coleman DJL, Allen CD, Heidenreich O, Fulton DA (2013) Determination of key structre-activity relationships in siRNA delivery with a mixed micelle system. J Control Release 172(3):939–945

Ozpolat B, Sood AK, Lopez-Berestein G (2010) Nanomedicine based approaches for the delivery of siRNA in cancer. J Intern Med 267(1):44–53

Modi P (2000) Mixed micellar delivery system and method of preparation. US Patent 6017545 A, 25 January 2000

Pérez SE, Gándola Y, Carlucci AM, González L, Turyn D, Bregni C (2012) Formulation strategies, characterization, and in vitro evaluation of lecithin-based nanoparticles for siRNA delivery. J Drug Deliv. Vol 2012, Article ID 986265, p 9, doi:10.1155/2012/986265

Schroeder A, Levins CG, Cortez C, Langer R, Anderson DG (2010) Lipid-based nanotherapeutics for siRNA delivery. J Intern Med 267(1):9–21

Shim MS, Kwon YJ (2010) Efficient and targeted delivery of siRNA in vivo. FEBS J 277(23):4814–4827

Smidt JH, Grit M, Crommelin DJA (1994) Dissolution kinetics of griseofulvin in mixed micellar solutions. J Pharm Sci 83:1209–1212

Spagnou S, Miller AD, Keller M (2004) Lipidic carriers of siRNA: differences in the formulation, cellular uptake, and delivery with plasmid DNA. Biochemistry 43(42):13348–13356

Sun Y, Miguéliz I, Navarro G, Tros de Ilarduya C (2009) Structural and morphological studies of cationic liposomes-DNA complexes. Lett Drug Des Discov 6:33–37

Sznitowska M, Klunder M, Placzek M (2008) Paclitaxel solubility in aqueous dispersions and mixed micellar solutions of lecithin. Chem Pharm Bull 56(1):70–74

Tan Y, Qi J, Lu Y, Hu F, Yin Z, Wu W (2013) Lecithin in mixed micelles attenuates the cytotoxicity of bile salts in Caco-2 cells. Toxicol In Vitro 27(2):714–720

Venneman NG, Huisman SJ, Moschetta A, van Berge-Henegouwen GP, van Erpecum KJ (2002) Effects of hydrophobic and hydrophilic bile salt mixtures on cholesterol crystallization in model biles. Biochim Biophys Acta 1583(2):221–228

Walter A, Vinson P, Kaplun A, Talmon Y (1991) Intermediate structures in the cholate-phosphatidylcholine vesicle-micelle transition. Biophys J 60:1315–1325

Walter A, Kuehl G, Barnes K, VanderWaerdt G (2000) The vesicle-to-micelle transition of phosphatidylcholine vesicles induced by nonionic detergents: effects of sodium chloride, sucrose and urea. Biochim Biophys Acta 1508:20–33

Wu SY, Singhania A, Burgess M et al (2011) Systemic delivery of E6/7 siRNA using novel lipidic particles and its application with cisplatin in cervical cancer mouse models. Gene Ther 18(1):14–22

Zamora MR, Budev M, Rolfe M, Gottlieb J, Humar A et al (2011) RNA interference therapy in lung transplant patients infected with respiratory syncytial virus. Am J Respir Crit Care Med 183:531–538

Zhao Q-Q et al (2009) N/P ratio significantly influences the transfection efficiency and cytotoxicity of a polyethylenimine/chitosan/DNA complex. Biol Pharm Bull 32(4):706–710